# TRANSIENT STABILITY IMPROVEMENT OF MULTI-MACHINE POWER SYSTEM USING UPFC TUNED-BASED PHASE ANGLE PARTICLE SWARM OPTIMIZATION

**G. El-Saady [1], \*, A. Ahmed [2], EL Noby [3] and M. A. Mohammed [4]**

*[1, 2, 3] Electrical Engineering Dept., Faculty of Engineering, Assiut University Assiut, Egypt*
*[4] Upper Egypt Electricity Distribution Company, Sohage, Egypt*

**ABSTRACT**

Optimal computation of parameters and placement of UPFC based minimization of New Voltage Stability Index (NVSI) are presented in this paper. The application of Unified Power Flow Controller (UPFC) to enhance transient stability of a multi-machine power system is listed. A supplementary stabilizer based on UPFC (like power system stabilizer) is designed to reach the defined purpose. Phase Angle Particle Swarm Algorithm (θ-PSO) is used as an optimization method. Several nonlinear time-domain simulation tests visibly show UPFC capability in damping of power system oscillations and consequently transient stability betterment. Comparisons based system transient stability enhancement among different UPFC locations and parameters are introduced. The effectiveness of the proposed method is analyzed with IEEE 14-bus and IEEE 30-bus test systems.

*Keywords:* Flexible AC Transmission System (FACTS), Unified Power Flow Controller (UPFC), Transient Stability, New Voltage Stability Index (NVSI), Phase Angle Particle Swarm Optimization (*θ*-PSO), Lead-Lag Power System Stabilizer (PSS), PI controllers.

## 1. Introduction

An electrical power system can be seen as the interconnection of generating sources and customer loads through a network of transmission lines, transformers, and ancillary equipment. [1]. Transient stability estimation of great power systems is an exceedingly intricate and greatly non-linear operation [2-4]. A major function of transient computation is to evaluate the ability of the power system to resist critical contingency in time, so that some emergencies or protective control can be applied to hinder system collapse [5]. In practical operations, correct assessment of transient stability for given operating states is necessary and valuable for power system operation [6].

Transient stability of a system refers to the stability when subjected to large disturbances such as faults and switching of lines [7]. The voltage stability, and steady state and transient

---

\* Corresponding author.
*E mail address:* gaber1@yahoo.com

stability of a complex power system can be effectively reformed by the use of FACTS devices [3-7].The transient stability of a generator depends on the difference between mechanical and electrical power [8-9]. During a fault, electrical power is reduced suddenly while mechanical power remains constant, thereby accelerating the rotor [10-11]. To maintain transient stability, the generator must transfer the exceeding power into the system. For this purpose, the existing FACTS devices can be employed.

Transient stability betterment by FACTS needs to the optimal computation of parameters and placement of FACTS, in this paper NVSI minimization [12-13] is chosen as an objective function for that.

In this paper a new strategy based PSO algorithm called $\theta$-PSO [14-16] which is based on phase angle vector but not the velocity vector [10], is firstly applied for optimal choice of the UPFC location and parameters in power systems.

FACTS devices [17-21] are capable of controlling the network condition in a very fast manner and this unique feature of FACTS devices can be exploited to enlarge the decelerating area and hence improving the first swing stability limit of a system. UPFC is member of FACTS family that is connected in shunt and series with the system [14].

In transient stability studies a load flow calculation is made first to obtain system conditions prior to disturbance. In this calculation, the network is composed of system buses, transmission lines and transformers. A transient stability analyzing is accomplished by joining a solution of the algebraic equations depicting the grid with a numerical solution of the differential equations. Transient stability analysis, fault analysis and rotor speed characteristics have been calculated without and with UPFC.

The modeling of UPFC is discussed in section 2. The equivalent model and formulation of NVSI are presented in section 3.The $\theta$-PSO is handled for tuning the parameters of UPFC, PI type controllers and lead-lag power system stabilizer (PSS). Results for the IEEE 14-bus and IEEE 30-bus power systems are discussed with respect to transient stability solution during the faults at different lines without and with UPFC device in section 8. Finally the conclusions are discussed in section 9**.**

## 2. Comprehensive mathematical modeling of UPFC controllers [14]

Fig (1) shows the basic circuit arrangement of UPFC where it consists of two switching converters. These converters are operated from a common DC link provided by a DC storage capacitor.
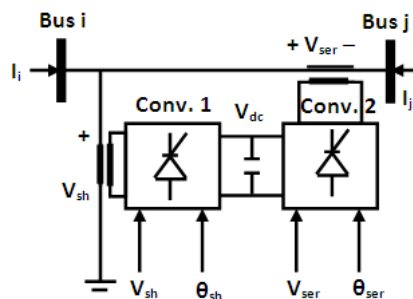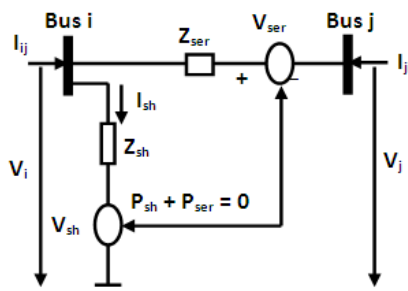


**Fig. 1.**UPFC operation principle.

**Fig. 2.**UPFC equivalent circuit.

According to the equivalent circuit shown in Fig (2), the power flow equations of the UPFC can be established:

$$P_{ij} = V_i^2 g_{ii} - V_i V_j (g_{ij} \cos(\theta_i - \theta_j) + b_{ij} \sin(\theta_i - \theta_j))$$
$$- V_i V_{ser} (g_{ij} \cos(\theta_i - \theta_{ser}) + b_{ij} \sin(\theta_i - \theta_{ser}))$$

$$- V_i V_{sh} (g_{sh} \cos(\theta_i - \theta_{sh}) + b_{sh} \sin(\theta_i - \theta_{sh})) \tag{1}$$

$$Q_{ij} = -V_i^2 b_{ii} - V_i V_j (g_{ij} \sin(\theta_i - \theta_j) - b_{ij} \cos(\theta_i - \theta_j))$$
$$- V_i V_{ser} (g_{ij} \sin(\theta_i - \theta_{ser}) - b_{ij} \cos(\theta_i - \theta_{ser}))$$

$$- V_i V_{sh} (g_{sh} \sin(\theta_i - \theta_{sh}) - b_{sh} \cos(\theta_i - \theta_{sh})) \tag{2}$$

$$P_{ji} = V_j^2 g_{jj} - V_i V_j (g_{ij} \cos(\theta_j - \theta_i) + b_{ij} \sin(\theta_j - \theta_i))$$

$$+ V_i V_{ser} (g_{ij} \cos(\theta_j - \theta_{ser}) + b_{ij} \sin(\theta_j - \theta_{ser})) \tag{3}$$

$$Q_{ji} = -V_j^2 b_{jj} - V_i V_j (g_{ij} \sin(\theta_j - \theta_i) - b_{ij} \sin(\theta_j - \theta_i))$$

$$+ V_i V_{ser} (g_{ij} \cos(\theta_j - \theta_{ser}) - b_{ij} \sin(\theta_j - \theta_{ser})) \tag{4}$$

Where, $g_{ij} + jb_{ij} = 1/Z_{ser}$, $g_{ii} = g_{ij} + g_{sh}$, $b_{ii} = b_{ij} + b_{sh}$, $g_{jj} = g_{ij}$, $b_{jj} = b_{ij}$.

The operating constraint of the UPFC (the active power exchange via the dc link) is

$$PE = P_{sh} + P_{ser} = 0 \tag{5}$$

Where, $P_{sh} = Re(V_{sh} I_{sh}^*)$ and $P_{sh} = Re(-V_{ser} I_{ji}^*)$

The bus voltage, the active power flow and the reactive power flow control as follows,

$$V_i - V_i^{Spec} \tag{6}$$

$$P_{ji} - P_{ji}^{Spec} \tag{7}$$

$$Q_{ji} - Q_{ji}^{Spec} \tag{8}$$

Where, $V_i^{Spec}$, $P_{ji}^{Spec}$ and $Q_{ji}^{Spec}$ are the specified bus voltage, line active and line reactive power flow.

## 3. The proposed new voltage stability index (NVSI) [12-13]

NVSI may be mathematically explained as follow [12].
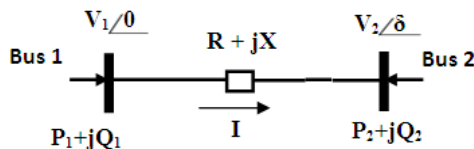
From Fig. 3 current flowing between bus 1 and 2,



**Fig. 3.** Line Model

$$I = \frac{V_1 \angle 0 - V_2 \angle \delta}{R + jX} \tag{9}$$

Comparatively resistance of the transmission line is negligible. The equation may be rewritten as:

$$\bar{I}^* = \frac{\overline{V_1}^* - \overline{V_2}^*}{jX} \tag{10}$$

And the receiving end power

$$S_2 = V_2 I^* \tag{11}$$

Incorporating Eq. 10 in 11 and solving

$$P_2 = - \left( \frac{V_1 V_2}{X} \right) \sin \delta \tag{12}$$

$$Q_2 = - \frac{V_2^2}{X} + V_1 V_2 \cos \delta \tag{13}$$

With eliminating δ from Eqs 12 & 13 yields

$$V_2^4 + (2Q_2 X - V_1^2) V_2^2 + X^2 (P_2^2 + Q_2^2) = 0 \tag{14}$$

This is an equation of order two of $V_2$. The condition to have at least one solution is:

$$(2Q_2 X - V_1^2)^2 - 4X^2 (P_2^2 + Q_2^2) \geq 0$$

$$\frac{2X \sqrt{(P_2^2 + Q_2^2)}}{(2Q_2 X - V_1^2)} \leq 1 \tag{15}$$

With taking the suffix "i" as the sending end bus & "j" as the receiving bus. NVSI can be defined by

$$NVSI_{ji} = \frac{2X \sqrt{(P_2^2 + Q_2^2)}}{(2Q_2 X - V_1^2)} \tag{16}$$

Where $P_j$ and $Q_j$ are the active and reactive powers at the receiving end bus, $V_i$ is the voltage magnitude at the sending end bus.

### 3.1. NVSI estimating procedure in the power systems [12]

The procedure to estimate the NVSI in all transmission lines in the power systems is shown in Fig. 4 [12]. The value of NVSI must be less than 1.00 in all transmission lines to maintain a stable system.
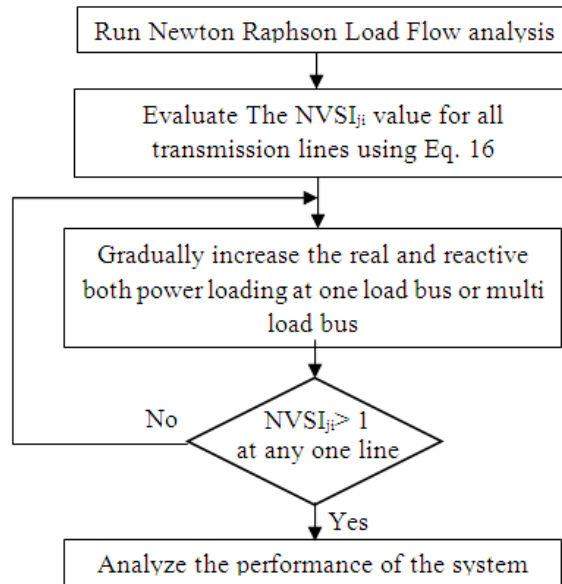
**Fig. 4.** Procedure for calculating $NVSI_{ji}$

## 4. θ- PSO technique [14-16]

The PSO method is a population-based one and is described by its developers as an optimization paradigm, which models the social behavior of birds flocking or fish schooling for food. Therefore, PSO works with a population of potential solutions rather than with a single individual [15]. The *θ*-PSO algorithm is newly introduced strategy of PSO which is a simple algorithm, easy to implement. It is based on phase angle vector instead of the velocity vector and an increment of phase angle $\Delta\theta_i$ vector replaces velocity vector $V_i$ which is dynamically adjusted according to the historical behaviors of the particle and its companions. In the *θ*-PSO, the positions are adjusted by the mapping of phase angles, thus, a particle is represented by its phase angle θ and increment of phase angle Δθ and its position decided by a mapping function [14]. The *θ*-PSO can be described with the following equations.

$$\Delta\theta_{id}(t+1) = w \times \Delta\theta_{id}(t) + c_1 r_1(\theta p_{id} - \theta_{id}(t)) + c_1 r_1 (\theta g_{gd} - \theta_{id}(t)) \qquad (17)$$

$$\theta_{id}(t+1) = \Delta\theta_{id}(t) + \Delta\theta_{id}(t+1) \qquad (18)$$

$$X_{id}(t) = f(\theta_{id}(t)) \qquad (19)$$

$$F'I(t) = \text{fitness value } (xi(t)) \qquad (20)$$

With,
$$\theta_{id}^{max} \geq \theta_{id} \geq \theta_{id}^{min}$$

$$\Delta\theta_{id}^{max} \geq \Delta\theta_{id} \geq \Delta\theta_{id}^{min}$$

$$X_{id}^{max} \geq X_{id} \geq X_{id}^{min}$$

The following inertia weight w is usually utilized in

$$w = w^{max} - \left(\frac{w^{max} - w^{min}}{iter^{max}}\right) * iter \qquad (21)$$

Where: $w^{max}$ and $w^{min}$ are the maximum and minimum inertia weight (0.9, 0.4). f is being a monotonic mapping function. In this paper,

$$f(\theta_{id}) = \frac{X^{max} - X^{min}}{2} \times \sin(\theta_{id}) + \frac{X^{max} + X^{min}}{2} \tag{22}$$

Where d=1, 2, …, D; i= 1, 2, …, S. The $\theta_{id}(t)$ is the phase angle of particle ith at time t; the $\Delta\theta_{id}(t)$ is the increment of particle i's phase angle at time t; $\theta p_{id}(t)$ is the phase angle of the personal best solution of particle i at time t; $\theta g_{gd}(t)$ is the phase angle of global best solution at time t; $F'_i(t)$ is the fitness value of particle i at time t which is identified by the function fitness value.

## 5. UPFC parameters optimization to improve NVSI of the system

In this section the following variables are considered as the optimization variables:

1. The series angle and voltage source ($V_{ser}$, $\theta_{ser}$) and the shunt angle and voltage source ($V_{sh}$, $\theta_{sh}$) for the UPFC are considered as the variables to be adjusted. The working range for these variables are [0.001 0.15] and [0 $2\pi$] for $V_{ser}$ and $\theta_{ser}$ respectively and [0.9 1.05] and [$\pi$ $-\pi$] for $V_{sh}$ and $\theta_{sh}$ respectively.
2. The main idea is that these variables are optimized indirectly by adjusting the active and reactive power desired and the bus voltage magnitude desired at a specified line. The aim of the optimization is to determine the critical line which is the most instability of the existing transmission lines. To verify the effectiveness and efficiency of the proposed $\theta$-PSO based $NVSI_{ji}$ minimization approach, the IEEE 14-bus and IEEE 30-bus power system are used as test systems. The numerical data for two test systems are taken from [22]. The simulation studies are carried out in MATLAB R2011b.Table 1 and Table 2 show $NVSI_{ji}$ of all the transmission lines of IEEE 14-bus and IEEE 30-bus after increasing of the two systems loads by 7 % and 16 % respectively without UPFC optimum parameters and with UPFC optimization parameters after locating it in the critical line. Table 3 and Table 4 show the UPFC optimum parameters.

**Table 1.**

NVSI$_{ji}$ of the transmission lines (IEEE 14-bus)

| Line No. | From bus i | To Bus j | NVSI$_{ji}$ Without UPFC | NVSI$_{ji}$ With UPFC |
|---|---|---|---|---|
| 1 | 1 | 2 | 0.2793 | 0.2474 |
| 2 | 1 | 5 | 1.0974 | 0.8591 |
| 3 | 2 | 3 | 0.0726 | 0.1886 |
| 4 | 2 | 4 | 0.0643 | 0.1621 |
| 5 | 2 | 5 | 0.0631 | 0.1587 |
| 6 | 3 | 4 | 0.3622 | 0.3179 |
| 7 | 4 | 5 | 0.0422 | 0.0389 |
| 8 | 4 | 7 | 0.1949 | 0.1806 |
| 9 | 4 | 9 | 0.5395 | 0.4975 |
| 10 | 5 | 6 | 0.0363 | 0.0340 |
| 11 | 6 | 11 | 0.0596 | 0.0448 |
| 12 | 6 | 12 | 0.0776 | 0.0581 |
| 13 | 6 | 13 | 0.0389 | 0.0295 |
| 14 | 7 | 8 | 0 | 0 |
| 15 | 7 | 9 | 0 | 0 |

| Line No. | From bus i | To Bus j | NVSI$_{ji}$ Without UPFC | NVSI$_{ji}$ With UPFC |
|---|---|---|---|---|
| 16 | 9 | 10 | 0.0544 | 0.0505 |
| 17 | 9 | 14 | 0.1691 | 0.1575 |
| 18 | 10 | 11 | 0.0388 | 0.0361 |
| 19 | 12 | 13 | 0.0244 | 0.0227 |
| 20 | 13 | 14 | 0.099 | 0.0919 |

**Table 2.**

NVSI$_{ji}$ of the transmission lines (IEEE 30-bus)

| Line No. | From bus i | To Bus j | NVSI$_{ji}$ Without UPFC | NVSI$_{ji}$ With UPFC |
|---|---|---|---|---|
| 1 | 1 | 2 | 0.3371 | 0.2745 |
| 2 | 1 | 3 | 1.0059 | 0.6537 |
| 3 | 2 | 4 | 0.1134 | 0.1227 |
| 4 | 3 | 4 | 0.0024 | 0.1381 |
| 5 | 2 | 5 | 0.1285 | 0.1241 |
| 6 | 2 | 6 | 0.1155 | 0.0020 |
| 7 | 4 | 6 | 0.0075 | 0.0064 |
| 8 | 5 | 7 | 0.2964 | 0.0357 |
| 9 | 6 | 7 | 0 | 0.2474 |
| 10 | 6 | 8 | 0 | 0 |
| 11 | 6 | 9 | 0 | 0 |
| 12 | 6 | 10 | 0 | 0 |
| 13 | 9 | 11 | 0 | 0 |
| 14 | 9 | 10 | 0 | 0 |
| 15 | 4 | 12 | 0.0417 | 0.1320 |
| 16 | 12 | 13 | 0.0374 | 0 |
| 17 | 12 | 14 | 0.0724 | 0 |
| 18 | 12 | 15 | 0.0381 | 0.0243 |
| 19 | 12 | 16 | 0.0566 | 0.0097 |
| 20 | 14 | 15 | 0.0281 | 0.0087 |
| 21 | 16 | 17 | 0.0166 | 0.0174 |
| 22 | 15 | 18 | 0.0419 | 0.0323 |
| 23 | 18 | 19 | 0.0098 | 0.0621 |
| 24 | 19 | 20 | 0.0154 | 0.0325 |
| 25 | 10 | 20 | 0.0287 | 0.0484 |
| 26 | 10 | 17 | 0.0114 | 0.0239 |
| 27 | 10 | 21 | 0.0103 | 0.0356 |
| 28 | 10 | 22 | 0.0205 | 0.0330 |
| 29 | 21 | 22 | 0.0109 | 0.0141 |
| 30 | 15 | 23 | 0.0389 | 0.0083 |
| 31 | 22 | 24 | 0 | 0.0131 |
| 32 | 23 | 24 | 0.0221 | 0.0093 |

| Line No. | From bus i | To Bus j | NVSI$_{ji}$ Without UPFC | NVSI$_{ji}$ With UPFC |
|---|---|---|---|---|
| 33 | 24 | 25 | 0.0801 | 0 |
| 34 | 25 | 26 | 0 | 0.0186 |
| 35 | 25 | 27 | 0 | 0.0682 |
| 36 | 28 | 27 | 0 | 0 |
| 37 | 27 | 29 | 0 | 0 |
| 38 | 27 | 30 | 0 | 0 |
| 39 | 29 | 30 | 0.0285 | 0 |
| 40 | 8 | 28 | 0.1574 | 0 |
| 41 | 6 | 28 | 0 | 0 |

**Table 3.**
Optimum UPFC location and parameters (IEEE 14-bus)

| UPFC line | UPFC parameters | | | |
|---|---|---|---|---|
| | $V_{sh}$ (p.u) | $\theta_{sh}$ (deg) | $V_{ser}$ (p.u) | $\theta_{ser}$ (deg) |
| 5-1 | 1.0353 | -11.1569 | 0.0693 | 238.8307 |

**Table 4.**
Optimum UPFC location and parameters (IEEE 30-bus)

| UPFC line | UPFC parameters | | | |
|---|---|---|---|---|
| | $V_{sh}$ (p.u) | $\theta_{sh}$ (deg) | $V_{ser}$ (p.u) | $\theta_{ser}$ (deg) |
| 3-1 | 1.031 | -10.757 | 0.148 | 201.43 |

From Tables 1 and 2 it can be conclude that the line No. 2 is the critical line in both of the two test systems and so the two systems stability is increased after connecting and optimizing of UPFC parameters in the critical line. Minimizing NVSI when be used as an objective function for determining the optimal location and parameters of UPFC increases the system transient stability this what will be seen in the following section.

## 6. The model of the multi-machine power system stability with UPFC

To establish a non-linear dynamic model of a multi-machine power system with UPFC installed [8], the UPFC model must be embeded into the power system model. Assume a UPFC is installed on a transmission line, line 1-2, as shown in Fig. 5.The following circuit equations can, thus be obtained.

$$V_1 = I_{sh} * X_{sh} + V_{sh} \tag{23}$$

$$V_2 = V_1 - I_{ser} * X_{ser} - V_{ser} \tag{24}$$

Equations (23) and (24) can be written in matrix form as follow,

$$\begin{bmatrix} \overline{V}_1 \\ \overline{V}_2 \end{bmatrix} = \begin{bmatrix} jX_{sh} & -jX_{sh} \\ jX_{sh} & j(X_{sh} + X_{ser} + X_L) \end{bmatrix} = \begin{bmatrix} \overline{I}_1 \\ \overline{I}_2 \end{bmatrix} + \begin{bmatrix} 1 & 0 \\ 1 & 1 \end{bmatrix} \begin{bmatrix} \overline{V}_{sh} \\ \overline{V}_{ser} \end{bmatrix} \tag{25}$$

Where: $I_1 = I_{sh} + I_{ser}, I_2 = I_{ser}$ and $X_L$ is the line reactance.

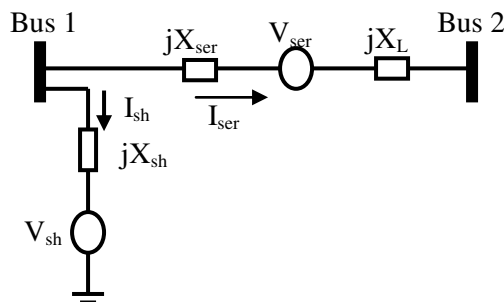**Fig. 5.** The circuit diagram of the UPFC installed in the transmission line

In short form, it can written Eq. 25 as

$$\overline{V}_{12} = \overline{A}.\overline{I}_{12} + \overline{B}.\overline{V}_{shser} \tag{26}$$

$$\overline{I}_{12} = \overline{A}^{-1}.\overline{V}_{12} - \overline{A}^{-1}.\overline{B}.\overline{V}_{shser} \tag{27}$$

Also, before UPFC is installed, it can be assumed that the network admittance matrix is $Y_r$, where only n generator nodes, plus nodes 1 and 2, are kept:

$$\begin{bmatrix} y_{11} & y_{12} & y_{1g} \\ y_{21} & y_{22} & y_{2g} \\ y_{g1} & y_{g2} & y_{gg} \end{bmatrix} \begin{bmatrix} \overline{V}_1 \\ \overline{V}_2 \\ \overline{V}_g \end{bmatrix} = Y_r \begin{bmatrix} \overline{V}_1 \\ \overline{V}_2 \\ \overline{V}_g \end{bmatrix} = \begin{bmatrix} 0 \\ 0 \\ \overline{I}_g \end{bmatrix} \tag{28}$$

Where, $\overline{I}_g$ and $\overline{V}_g$ are the generators' current and internal voltage vector.

With installation of UPFC on line 1-2, the network Eq. 28 can be written as:

$$\begin{bmatrix} y_{11} & y_{12} & y_{1g} \\ y_{21} & y_{22} & y_{2g} \\ y_{g1} & y_{g2} & y_{gg} \end{bmatrix} \begin{bmatrix} \overline{V}_1 \\ \overline{V}_2 \\ \overline{V}_g \end{bmatrix} + \begin{bmatrix} 1 & 0 \\ 0 & -1 \\ 0 & 0 \end{bmatrix} \begin{bmatrix} \overline{I}_1 \\ \overline{I}_2 \end{bmatrix} = \begin{bmatrix} 0 \\ 0 \\ \overline{I}_g \end{bmatrix} \tag{29}$$

By substituting Eq. 27 into Eq. 29 and making a partition to eliminate nodes 1 and 2 in Eq. 29, it can be obtained that:

$$\begin{bmatrix} \overline{Y}_1 & \vdots & \overline{Y}_2 \\ ---&\vdots&--- \\ \overline{Y}_3 & \vdots & \overline{Y}_4 \end{bmatrix} \begin{bmatrix} \overline{V}_{12} \\ --- \\ \overline{V}_g \end{bmatrix} + \begin{bmatrix} C \\ - \\ 0 \end{bmatrix} [\overline{A}^{-1}.\overline{V}_{12} - \overline{A}^{-1}.\overline{B}.\overline{V}_{shser}] = \begin{bmatrix} 0 \\ - \\ \overline{I}_g \end{bmatrix} \tag{30}$$

By using the Keron elimination method, nodes 1 and 2 can be deleted. Consequently, it is found that:

$$\overline{I}_g = \overline{Y}_g\overline{V}_g + \overline{Y}_U\overline{V}_{shser} \tag{31}$$

Where:

$$C = \begin{bmatrix} 1 & 0 \\ 0 & -1 \end{bmatrix}$$

$$\overline{Y}_g = \overline{Y}_4 - \overline{Y}_3(\overline{Y}_1 + C\,\overline{A}^{-1})^{-1}\overline{Y}_2$$

$$\overline{Y}_U = -\overline{Y}_3(\overline{Y}_1 + C\,\overline{A}^{-1})^{-1}C\,\overline{A}^{-1}\overline{B}$$

The electrical power output of each machine can now be expressed in the machine's internal voltages as follow:

$$P_{ei} = \text{Re}(\overline{V}_{gi}\overline{I}_{gi}) \tag{32}$$

$$\overline{I}_{gi} = \sum_{j=1}^{m} \overline{V}_{gj}\overline{Y}_{ij} + \overline{Y}_{Ui}\overline{V}_{shseri} \tag{33}$$

Where m is number of machines, $Y_{ij}$ are the elements of $Y_g$matrix, $Y_{Ui}$ are the elements of $Y_U$ matrix and $V_{shseri}$ are the elements of $V_{shser}$matrix.

Expressing voltages and admittances in polar form, i.e. $V_{gi} = |V_{gi}| \angle \delta_i, Y_{ij} = |Y_{ij}| \angle \theta_{ij}, Y_{Ui} = |Y_{Ui}| \angle \theta_{Ui}$ and $V_{shseri} = |V_{shseri}| \angle \delta_{shseri}$ and substituting for $I_{gi}$ in Eq. (33), result in

$$P_{ei} = \sum_{j=1}^{m} |V_{gi}||V_{gj}| |Y_{ij}| \cos(\theta_{ij} - \delta_i + \delta_j) + |V_{gi}||Y_{Ui}||V_{shseri}| \cos(\theta_{Ui} - \delta_i \delta_{shseri}) \quad (34)$$

The above equation is the same as the power flow equation. Prior to disturbance, there is equilibrium between the mechanical power input and the electrical power output, and we have

$$P_{mi} = P_{ei} \tag{35}$$

The classical transient stability study is based on the application of a three-phase fault. A solid three-phase fault at bus k in the network results in $V_k = 0$. This is simulated by removing the kth row and column from the prefault bus admittance matrix. The new bus admittance matrix is reduced by eliminating all nodes except the internal generator nodes. The generator excitation voltages during the fault and postfault modes are assumed to remain constant. The electrical power of the ith generator in terms of the new reduced bus admittance matrices are obtained from (34).The swing equation for machine i becomes

$$\frac{H_i}{\pi f_o} \frac{\partial^2 \delta_i}{\partial t^2} = \left( \Delta P_{mi} - \Delta P_{ei}^f - D_i \, \Delta \omega_i \right) \tag{36}$$

Where $H_i$ is the inertia constant, $P_{ei}^f$ the electrical power during or post fault, $\omega_i$ rotor speed and $D_i$ damping constant all of the machine i. $f_o$ the base frequency of the system.

Showing the electrical power of the ith generator by $P_e^f$ and transforming Eq. (36) into state variable mode yields

$$\frac{\partial \delta_i}{\partial t} = \omega_o \Delta \omega_i \tag{37}$$

$$\frac{\partial \Delta \omega_i}{\partial t} = \frac{\pi f_o}{H_i} \left( \Delta P_{mi} - \Delta P_{ei}^f - D_i \, \Delta \omega_i \right) \tag{38}$$

In transient stability analysis problem, the authors have the second state equation for each generator. When the fault is cleared, which may involve the removal of the faulty line, the bus admittance matrix is recomputed to reflect the change in the networks. Next the post fault reduced bus admittance matrix is evaluated and the post fault electrical power of the ith generator is readily determined from Eq. (34).

## 7. Design of damping and internal UPFC controllers parameters

UPFC has two internal controllers which are Bus voltage controller and DC voltage regulator. In this paper PI type controllers are considered for UPFC control problem. Fig. 6 shows the structure of the bus voltage controller and DC voltage regulator. A power system stabilizer is provided to improve the damping of power system oscillations and stability enhancement. This stabilizer is commonly designed as a lead-lag compensator. This stabilizer aims to provide an electrical torque in phase with the speed deviation whereupon the damping of power system oscillations is enhanced. The transfer function

model of the stabilizer is shown in Fig. 7. It consists of gain ($K_{ps}$), signal washout filter and phase compensator block respectively.
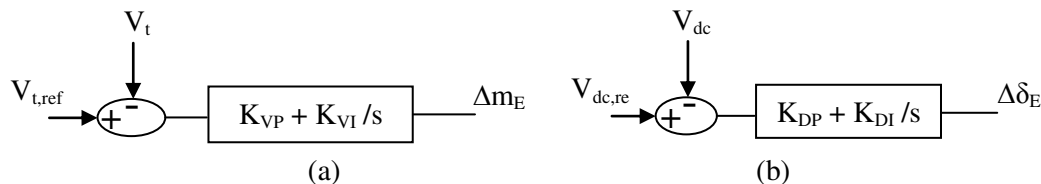


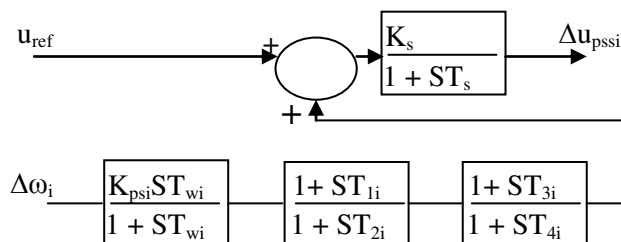**Fig. 6.** (a) Bus voltage controller and (b) DC voltage regulator



**Fig. 7.** Lead-lag power system Stabilizer

Where:

$K_P$ and $K_I$ are the proportional and integral gains, $m_E$ and $\delta_E$ are the excitation amplitude modulation ratio and the excitation phase angle respectively.

A linear dynamic model of the system with UPFC is obtained as follows:

$$\Delta\dot{\omega}_i = \frac{\Delta P_{mi} - \Delta P_{ei} - D_i\,\Delta\omega_i}{M_i}$$

$$\Delta\dot{\delta} = \omega_o \Delta\omega_i$$

$$\Delta\dot{P}_{ei} = K_{1i}\,\Delta\delta_i + K_{pdi}\,\Delta V_{dc} + K_{pei}\,\Delta m_E + K_{p\delta ei}\,\Delta\delta_E \qquad (38)$$

$$\Delta\dot{V}_{ti} = K_{2i}\,\Delta\delta_i + K_{vdi}\,\Delta V_{dc} + K_{vei}\,\Delta m_E + K_{v\delta ei}\,\Delta\delta_E$$

$$\Delta\dot{V}_{dc} = K_{3i}\,\Delta\delta_i + K_{4i}\,\Delta V_{dc} + K_{cei}\,\Delta m_E + K_{c\delta ei}\,\Delta\delta_E$$

$M_i$ is the moment of inertia of the generator i. The constant parameters denoted by K are function of the system parameters and the initial operating condition.

The state-space equations of the system can be obtained from equation (38) as follows:

$$\dot{X} = AX + BU$$

$$X = [\Delta\delta_i \Delta\omega_i\,\Delta V_{dc}]^t \qquad (39)$$

$$U = [\Delta u_{pssi}\,\Delta m_E\,\Delta\delta_E]^t$$

Where, A and B matrices of the system are defined as follows:

$$A = \begin{bmatrix} 0 & \omega_o & 0 \\ \dfrac{-K_{1i}}{M_i} & \dfrac{-D_i}{M_i} & \dfrac{-K_{pdi}}{M_i} \\ K_{3i} & 0 & -K_{4i} \end{bmatrix} \qquad B = \begin{bmatrix} 0 & 0 & 0 \\ 0 & \dfrac{-K_{pei}}{M_i} & \dfrac{-K_{p\delta ei}}{M_i} \\ 0 & K_{cei} & K_{c\delta ei} \end{bmatrix} \qquad (40)$$

As mentioned before, PI type controllers are designed for UPFC in addition to stabilizer controller. These controllers are tuned using $\theta$-PSO. Often, the closed-loop modes are specified to have some degree of relative stability. In this case, the closed loop eigen values are constrained to lie to the left of a vertical line corresponding to a specified damping factor. To satisfy this case the parameters of the damping and PI controllers may be selected to minimize the following objective function [7]:

$$J = \sum_{\sigma_i \geq \sigma_o} \sigma_i - \sigma_o \qquad (41)$$

$\sigma_o$ represents the desirable level of the system damping. This level can be achieved by shifting the dominant Eigen values to the left of s $=\sigma_o$ line in the s-plane. This also ensures some degree of relative stability. The condition $\sigma_i \geq \sigma_o$ is imposed on the evaluation of J to consider only the unstable or poorly damped modes that mainly belong to the electromechanical ones. The relative stability is determined by the value of $\sigma_o$. This will place the closed-loop Eigen values in a sector in which $\sigma_i \leq \sigma_o$ as shown in Fig. 8.
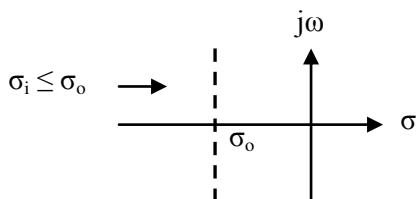


**Fig. 8.** Region of Eigen values location for J

The design problem can be formulated as the following constrained optimization problem, where the constraints are the controller parameters bounds:

Minimize *J* subject to:

$$K^{min} \leq K \leq K^{max}$$
$$T_w^{min} \leq T_w \leq T_w^{max} \qquad (42)$$
$$T_i^{min} \leq T_i \leq T_i^{max}$$

Where K describes all K parameters of damping and PI controllers and its typical ranges are [– 100, 100]. $T_w$ is a filter constant, it is generally taken between 0.01 s to 20 s. $T_i$ are a phase compensator block constants where i = 1,2,3,4 and their typical ranges are [0.01, 5]. The proposed approach employs $\theta$-PSO algorithm to solve this optimization problem. In order to acquire better performance the input parameters that control the $\theta$-PSO, i.e., number of particle, the number of iteration, $c_1$ and $c_2$ are chosen as 30, 60, 2.1 and 2.1, respectively.

## 8. Simulation result

In order to study and analyze the system performance with UPFC when the minimization of NVSI is used as an objective function based optimum UPFC and PSS

parameters on the transient stability two scenarios are considered in IEEE 14-bus and IEEE 30-bus systems as follow:

**First IEEE 14-bus:**

Scenario 1:3-phase symmetrical short circuit fault of 400 milli-seconds duration (Tc) occurs at the bus 10 which the line 10-9 is the faulty line.

Scenario 2:3-phase symmetrical short circuit fault of 200 milli-seconds duration (Tc) occurs at the bus 12 which the line 12-13 is the faulty line.

Four cases will be studied in each scenario as follow:

**Case 1:** optimum parameters and location of UPFC according to Table 3 based minimization of NVSI.

**Case 2:** optimum location of UPFC according to Table 1 but random UPFC parameters according to Table 5.

**Table 5.**
case 2

| Optimum UPFC line | Random UPFC parameters | | | |
|---|---|---|---|---|
| | $V_{sh}$ (p.u) | $\theta_{sh}$ (deg) | $V_{ser}$ (p.u) | $\theta_{ser}$ (deg) |
| 5-1 | 0.9951 | -12.2 | 0.1366 | 239.48 |

**Case 3:** random UPFC location and parameters according to Table 6.

**Table 6.**
case 3

| Random UPFC line | Random UPFC parameters | | | |
|---|---|---|---|---|
| | $V_{sh}$ (p.u) | $\theta_{sh}$ (deg) | $V_{ser}$ (p.u) | $\theta_{ser}$ (deg) |
| 4-3 | 0.9859 | -10.1 | 0.039 | 156.33 |

**Case 4:** the system without UPFC.

Fig. 9 until Fig. 13 show generators speed deviation of IEEE 14-bus system of four cases in the first scenario. Fig. 14 until Fig. 18 show generators speed deviation of IEEE 14-bus system of four cases in the second scenario. The system is simulated in MATLAB R2011b.
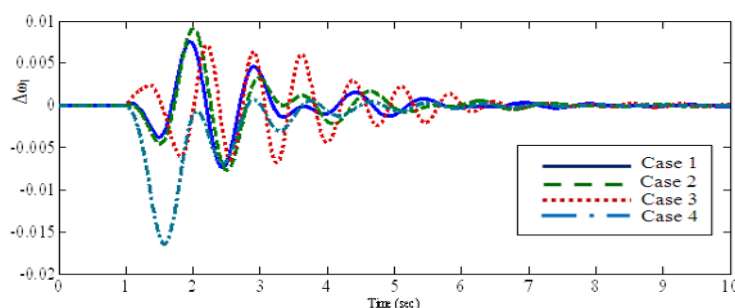


**Fig. 9.** Rotor speed deviation of G1 (Scenario 1)

Oscillation damping of the G1 speed is smooth and fast with case 1. The transient stability of G1 is the best with UPFC.
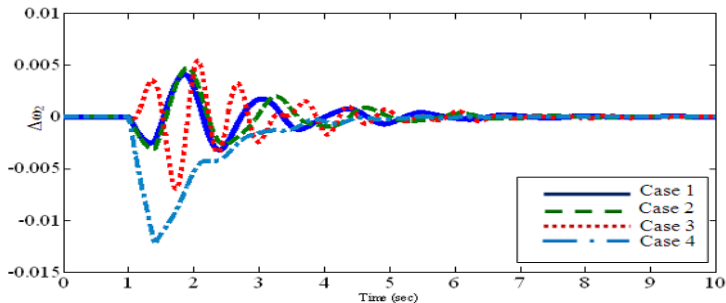
**Fig. 10.** Rotor speed deviation of G2 (Scenario 1)

As it is seen in Fig. 10 case 1 gives the best response among the other cases with G2.
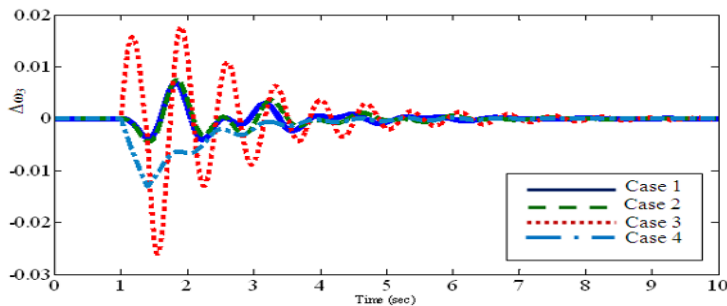


**Fig. 11.** Rotor speed deviation of G3 (Scenario 1)

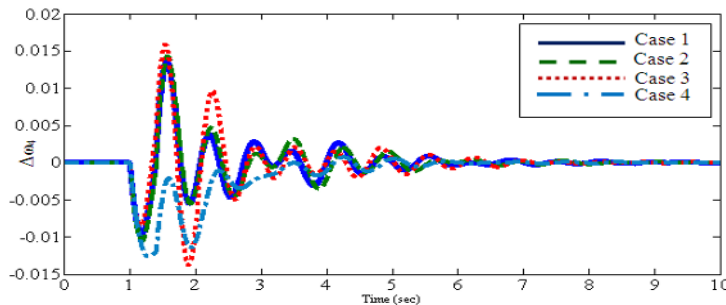Fig. 11 shows that case 3 is the worst and the effect of case 1 and case 2are the same and the best for G3.



**Fig. 12.** Rotor speed deviation of G4 (Scenario 1)

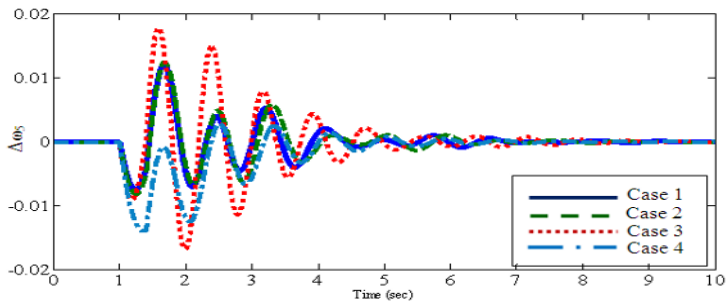It is explicated from Fig. 12 that case 3 is still the worst among the cases.



**Fig. 13.**Rotor speed deviation of G5 (Scenario 1)

Fig. 13 shows case 1 and case 2 are alike. Responses of cases 1, 2 and 4 settle after the time 4 second but case 3 settles after the time 5 second.

From scenario 1 of IEEE 14-bus, optimum parameters and location of UPFC based minimization of NVSI (case 1) gives the best response of the transient stability while the UPFC random parameters and location present bad response.
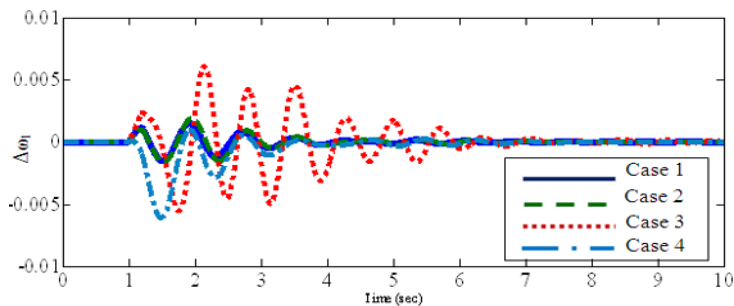


**Fig. 14.** Rotor speed deviation of G1 (Scenario 2)
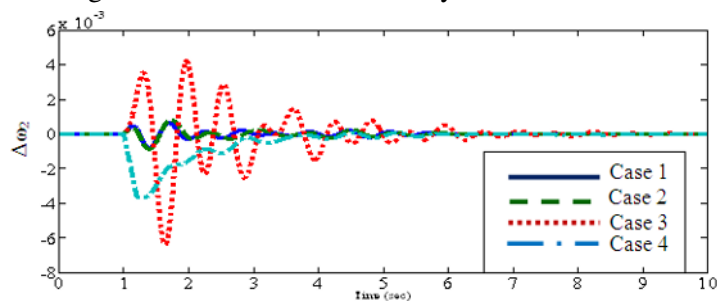
It is cleared from Fig. 14 case 3 doesn't release any reform with G1.



**Fig. 15.** Rotor speed deviation of G2 (Scenario 2)

Clearly the transient stability of G2 is improved with cases 1 and 2. Fig. 15 explains that.
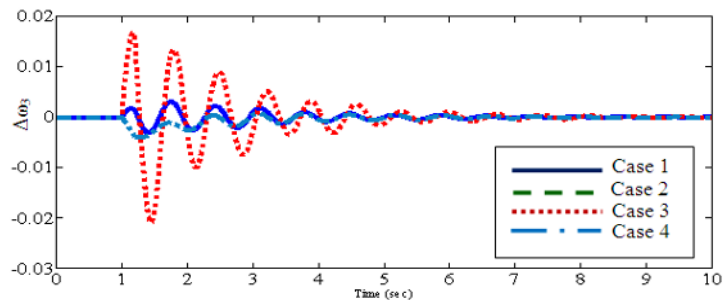


**Fig. 16.** Rotor speed deviation of G3 (Scenario 2)
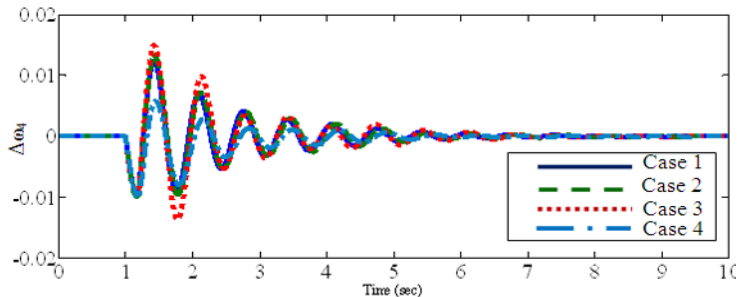
Fig. 16 presents that case 1, 2 and 3 are the best for G3.

**Fig. 17.** Rotor speed deviation of G4 (Scenario 2)

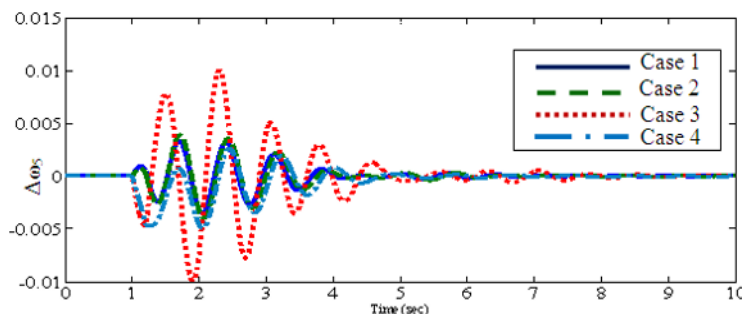Transient stability become well with case 4 for G4, this is visible from Fig. 17.



**Fig. 18.** Rotor speed deviation of G5 (Scenario 2)

From Fig. 18 it can be conclude that case 3 is the worst with G5.

Scenarios 1 and 2 when are applied IEEE 14-bus, confirm on an important UPFC optimal and location based NVSI minimization (case 1). This result needs an affirmation so two scenarios are applied IEEE 30-bus; this is studied in the following section.

**Second IEEE 30-bus:**

Scenario 1:3-phase symmetrical short circuit fault of 400 milli-seconds duration (Tc) occurs at the bus 15 which the line 15-14 is the faulty line.

Scenario 2:3-phase symmetrical short circuit fault of 600 milli-seconds duration (Tc) occurs at the bus 25 which the line 25-27 is the faulty line.

The previous four cases will be studied in each scenario as follow:

**Case 1:** optimum parameters and location of UPFC according to Table 5 based minimization of NVSI.

**Case 2:** optimum location of UPFC according to Table 2 but random UPFC parameters according to Table 7.

**Table 7.**

case 2

| Optimum UPFC line | Random UPFC parameters | | | |
|---|---|---|---|---|
| | $V_{sh}$ (p.u) | $\theta_{sh}$ (deg) | $V_{ser}$ (p.u) | $\theta_{ser}$ (deg) |
| 3-1 | 0.961 | -10.68 | 0.117 | 337.171 |

**Case 3:** random UPFC location and parameters according to Table 8.

**Table 8.**
case 3

| Random UPFC line | Random UPFC parameters | | | |
|---|---|---|---|---|
| | $V_{sh}$ (p.u) | $\theta_{sh}$ (deg) | $V_{ser}$ (p.u) | $\theta_{ser}$ (deg) |
| 7-5 | 1.0186 | -12.688 | 0.0172 | 352.855 |

**Case 4:** the system without UPFC.

Fig. 19 until Fig. 24 show generators speed deviation of IEEE 30-bus system of four cases in the first scenario. Fig. 25 until Fig. 30 show generators speed deviation of IEEE 30-bus system of four cases in the second scenario. The system is simulated in MATLAB R2011b.
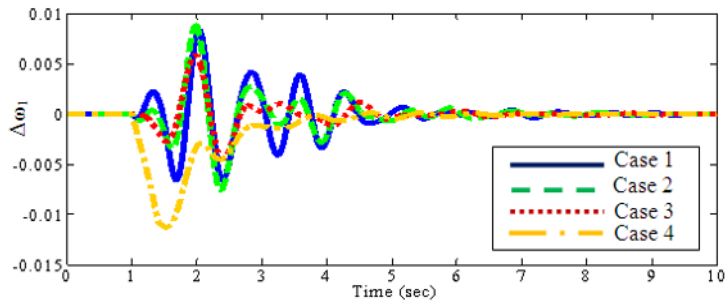
**Fig. 19.** Rotor speed deviation of G1 (Scenario 1)

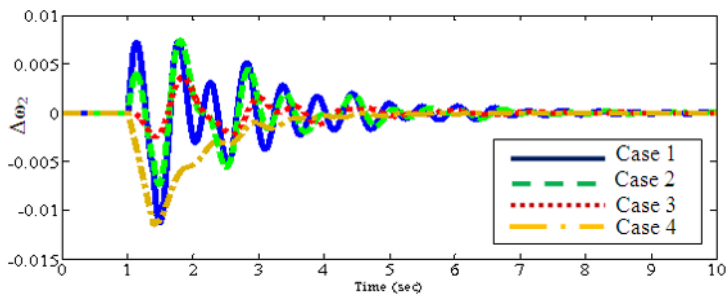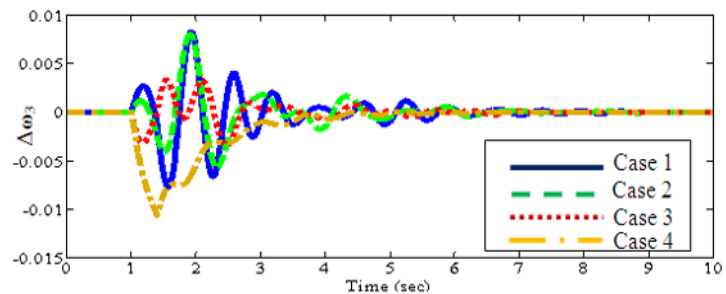Case 3 with G1 is the best this is observed from Fig. 19.

**Fig. 20.** Rotor speed deviation of G2 (Scenario 1)

Fig. 20 clears case 3 realizes a response is better than the other cases.

**Fig. 21.** Rotor speed deviation of G3 (Scenario 1)

G3 with the system without UPFC gives a response of transient stability is the worst in addition to case 1 doesn't present the best. This is obvious from Fig. 21.
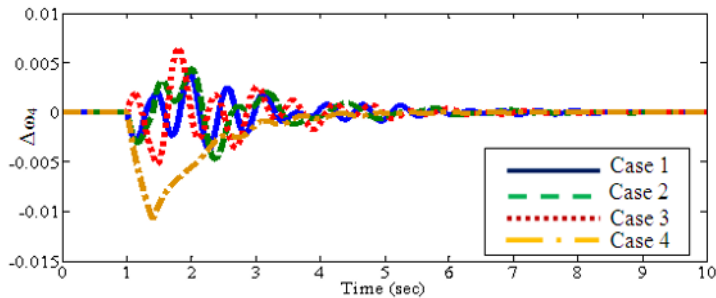
**Fig. 22.**Rotor speed deviation of G4 (Scenario 1)

From Fig. 22 it is distinct that case 1 actualizes a response which is the least among the studied cases for G4.
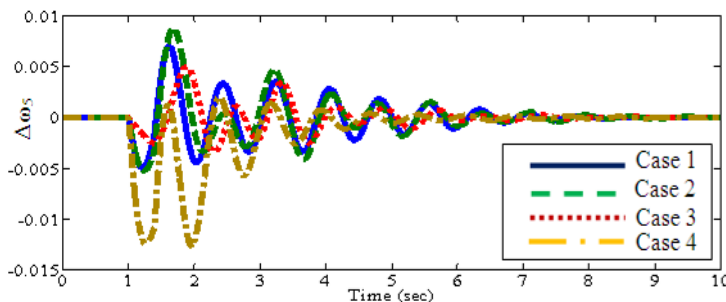


**Fig. 23.** Rotor speed deviation of G5 (Scenario 1)

It can be deduced from Fig. 23 that case 3 better appears and case 1 is better than case 2 as well as case 4 is unwanted for G5.
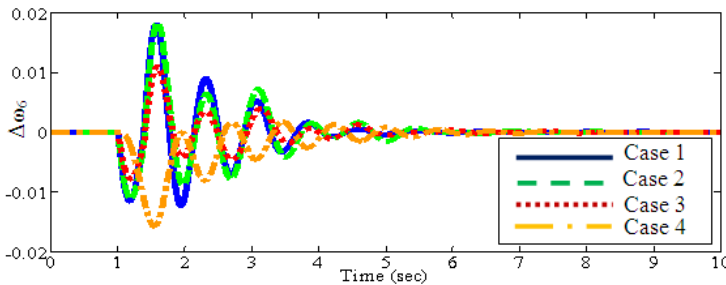


**Fig. 24.** Rotor speed deviation of G6 (Scenario 1)

Fig. 24 illustrates that G6 transient stability with case 3 becomes better.

Many concepts can be figured out from applying scenario 1 on IEEE 30-bus as follow:

1. Case 3 achieves transient stability is the best with all system generators except G4.
2. Case 1 can't execute the expected target which is the best case.
3. System transient stability is reformed with UPFC.

In the following section scenario 2 as mentioned before is applied on IEEE 30-bus.
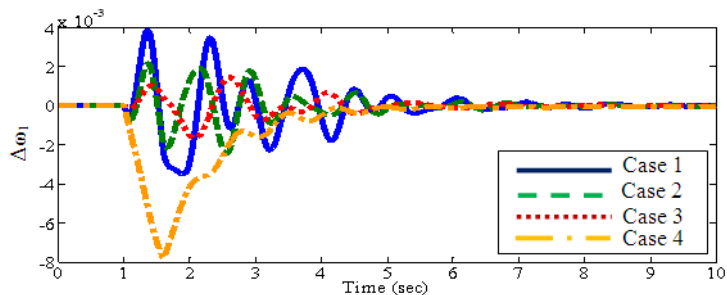
**Fig. 25.** Rotor speed deviation of G1 (Scenario 2)

Case 1 and case 2 can't attain any progress with G1; this can be remarked from Fig. 25 and also G1 transient stability gains badness with case 4.
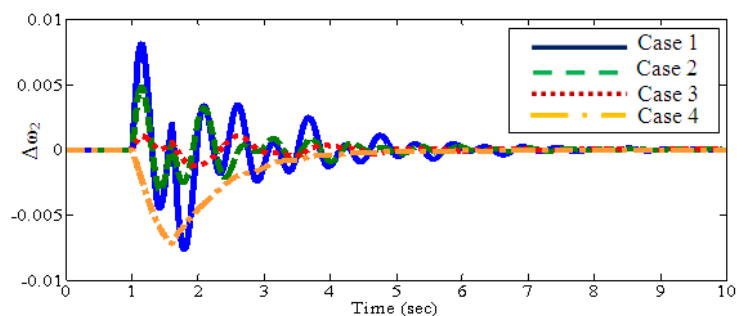


**Fig. 26.** Rotor speed deviation of G2 (Scenario 2)

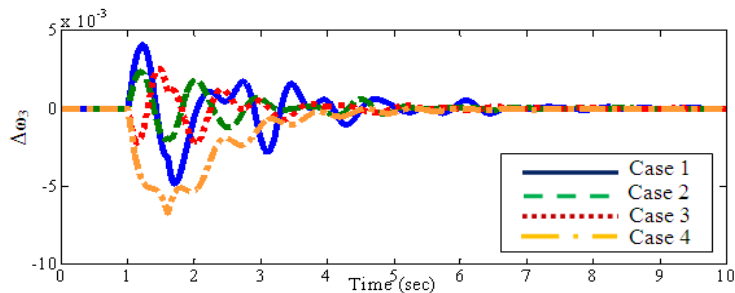Fig. 26 makes apparent that case 1 with G2 is the worst.



**Fig. 27.** Rotor speed deviation of G3 (Scenario 2)

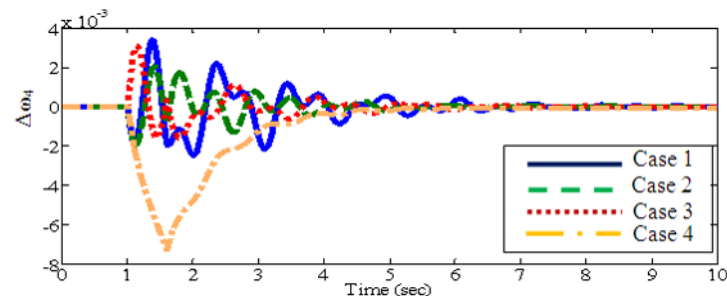What can be understand from Fig. 27 that case 2 and case 3 become less response.



**Fig. 28.** Rotor speed deviation of G4 (Scenario 2)

From Fig. 28 it is noted that G4 transient stability improves with case 2 and case 3.
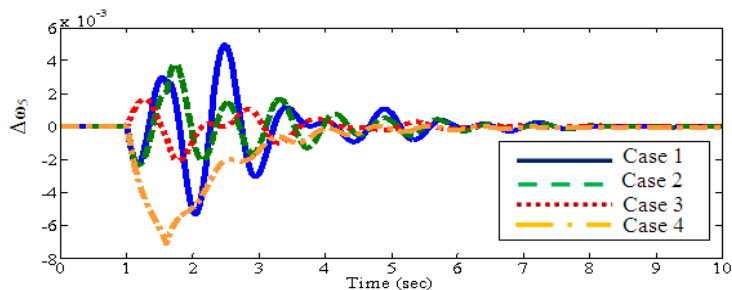


**Fig. 29.** Rotor speed deviation of G5 (Scenario 2)

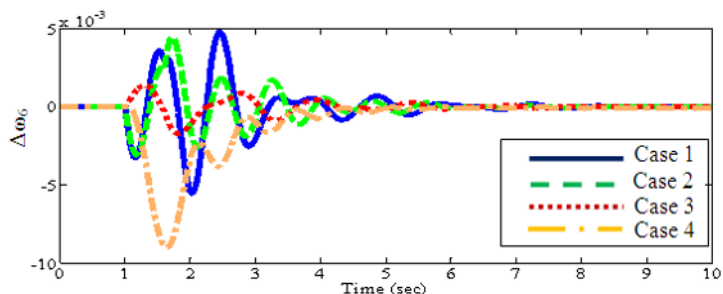Fig. 29 highlights that case 3 still gives the good response with G5.



**Fig. 30.** Rotor speed deviation of G6 (Scenario 2)

It can be inferred from Fig. 30 that case 3 with G6 actualizes the best result.

After applying two scenarios on two different power systems for testing UPFC location and parameters capability to improve the two system transient stability, it can be shortened the results as follow:

1- Optimizing of UPFC location and parameters based NVSI minimization reforms the system capacity towards betterment the stability of the weakest bus and line with load growth.

2- The above mentioned outcome can meliorate the transient stability of all IEEE 14 bus generators with applying the aforementioned scenarios of 3-phase symmetrical short circuit fault.

3- With IEEE 30-bus system the first mentioned result doesn't realize the best case contrariwise the random UPFC location and parameters presents the preferable effect except with G4.

4- Minimization of NVSI as an objective function for optimizing of UPFC location and parameters is unreliable for amelioration the system transient stability.

5- UPFC play an important role for betterment the system transient stability provided the optimal election of its location and parameters.

The parameters of PI controller are designed based case 1 this shown in Table 9 and the parameters of the power system stabilizer (PSS) are designed based cases 1 and 4 respectively this presented in Tables 10 and 11 all are tuned using $\theta$-PSO.

**Table 9.**

Optimum parameters of PI controller

| With IEEE 14-bus system | | | | With IEEE 30-bus system | | | |
|---|---|---|---|---|---|---|---|
| $K_{DP}$ | $K_{DI}$ | $K_{VP}$ | $K_{VI}$ | $K_{DP}$ | $K_{DI}$ | $K_{VP}$ | $K_{VI}$ |
| -100 | -100 | -11.596 | -100 | 11.59 | 100 | -100 | 100 |

**Table 10.**

Optimum parameters of PSS with IEEE 14-bus system

| Par | With UPFC (case 1) | | | | | Without UPFC (case 4) | | | | |
|---|---|---|---|---|---|---|---|---|---|---|
| | $G_1$ | $G_2$ | $G_3$ | $G_4$ | $G_5$ | $G_1$ | $G_2$ | $G_3$ | $G_4$ | $G_5$ |
| $K_{ps}$ | -100 | 24.8 | 90.7 | 67.4 | 100 | 23.02 | -62.5 | -7.42 | -77.8 | 16.23 |
| $T_1$ | 0.01 | 1.76 | 0.01 | 5 | 5 | 2.664 | 1.29 | 3.96 | 0.16 | 3.098 |
| $T_2$ | 5 | 4.63 | 0.01 | 0.01 | 5 | 4.731 | 2.59 | 4.87 | 2.25 | 2.199 |
| $T_3$ | 4.96 | 5 | 5 | 0.01 | 0.01 | 2.279 | 2.35 | 3.55 | 0.42 | 1.85 |
| $T_4$ | 1.81 | 4.17 | 0.33 | 0.27 | 5 | 0.815 | 2.78 | 1.27 | 0.78 | 2.272 |
| $T_w$ | 0.01 | 20 | 0.01 | 0.01 | 0.01 | 13.47 | 10.9 | 12.7 | 6.15 | 12.07 |

**Table 11.**

Optimum parameters of PSS with IEEE 30-bus system

| Par | With UPFC (case 1) | | | | | | Without UPFC (case 4) | | | | | |
|---|---|---|---|---|---|---|---|---|---|---|---|---|
| | $G_1$ | $G_2$ | $G_3$ | $G_4$ | $G_5$ | G6 | $G_1$ | $G_2$ | $G_3$ | $G_4$ | $G_5$ | G6 |
| $K_{ps}$ | -100 | 67.5 | 100 | 98.7 | 58.9 | -100 | -15.4 | -85.9 | 6.3 | -95.1 | 37.5 | 8.74 |
| $T_1$ | 4.96 | 5.00 | 5.00 | 1.27 | 0.01 | 0.043 | 0.36 | 3.17 | 0.15 | 0.56 | 1.08 | 1.95 |
| $T_2$ | 0.01 | 5.00 | 0.01 | 0.01 | 0.01 | 5.00 | 0.6 | 2.56 | 3.35 | 0.05 | 0.96 | 0.03 |
| $T_3$ | 0.01 | 5.00 | 0.01 | 5.00 | 0.01 | 0.048 | 3.03 | 4.1 | 1.64 | 4.99 | 3.15 | 4.6 |
| $T_4$ | 5.00 | 0.01 | 0.01 | 0.01 | 0.01 | 5.00 | 2.06 | 2.3 | 3.6 | 2.1 | 0.14 | 4.9 |
| $T_w$ | 20.0 | 0.01 | 0.01 | 20.0 | 0.01 | 0.011 | 2.72 | 13.9 | 14.2 | 6.87 | 0.18 | 18.1 |

The system eigen values based cases 1 and 4 according to the objective function (Eq. 41) are given in Tables 11 and 12.

**Table 12.**

System eigen values (IEEE 14-bus system)

| Without UPFC (case 4) | With UPFC (case 1) |
|---|---|
| -100, -0.51, -1.5, -0.4, -100, -0.4, -0.07, -100, -0.3, -0.3, -0.07, -100, -0.48, -1.97, -0.15, -100, -6, -0.95, -1.2, -0.40 ± j 10.71, -0.47 ± j 9.09, -0.44 ± j 8.6, -0.49 ± j7.3, -0.001, -0.89 | -100, -100, -0.2, -100, -100, -0.05, -100, -100, -100, -100, -0.2, -100, -100, -100, -0.2, -100, -100, -100, -100, -0.05, -0.55 ± 10.97, -0.63 ± j5.07, -0.67 ± j9.55, -0.60 ± j9.01, -0.69 ± j7.68, -97.07 ± j19.48, -1.99 ± j0.17 |

**Table 13.**

System eigen values (IEEE 30-bus system)

| Without UPFC (case 4) | With UPFC (case 1) |
|---|---|
| -100, -0.49, -1.6, -0.37, -100, -0.44, -0.39, -0.07, -100, -0.28, -0.3, -0.07, -100, -0.48, -21.22, -0.15, -100, -6.94, -1.04, -1.20,-100, -0.2, -37.8, -0.06, -0.001,  -1.3,  -0.57 ± j11.1, -0.64 ± j10.26, -0.68 ± j7.3, -0.6 ± 8.7,-0.69 ± j8.2, | -100, -100, -0.2, -8.12, -100, -100, -100, -100, -100, -100, -100, -100, -100, -100, -100, -100, -100, -5.00, -0.56 ± j11.67, -0.66 ± j10.79, -0.64 ± j5.3, -0.59 ± j9.3, -0.69 ± j8.6, -0.68 ± j7.9, -0.28 ± j0.58, -19.2 ± j5.4, |

## 9. Conclusion

Mathematical models for simultaneously optimizing location and parameters of UPFC based the stability index is minimized are presented in this paper. The paper has developed a notable advantage by introducing the new voltage stability index (NVSI). The index has been implemented in the comprehensive Newton-Raphson load flow method. The merits of the index are that it relates both real and reactive power of the system. A Phase Angle Particle Swarm Optimization Algorithm is used to solve this nonlinear programming problem. The cases study of the IEEE 14-bus and IEEE 30-bus systems have confirmed that the developed algorithm is correct and effective. This paper has proposed a procedure for optimal control co-ordination design of PSSs and UPFC devices in a multi-machine power system. The control coordination problem is solved through the application of constrained optimization method. The procedure is based on the use of the $\theta$-PSO which adjusts the parameters of the controllers to achieve system stability and maintain optimal damping as the system operating condition and/or configuration change. The simulation results proved that the power system is more stable with UPFC device provided the optimal choice of its location and parameters.

### REFERENCES

[1] Prabha Kundur, John Paserba, "Definition and Classification of Power System Stability", IEEE Trans. on Power Systems., Vol. 19, No. 2, pp 1387- 1401, May 2004.

[2] Prechanon Kumkratug,"Application of UPFC to increase Transient Stability of Inter-Area Power System", Journal of Computers, vol.4. No.4, April 2009

[3] Manish Kumar Saini, Naresh Kumar Yadav, Naveen Mehra," Transient Stability Analysis of Multi-machine Power System with FACT Devices using MATLAB/Simulink Environment", International Journal of Computational Engineering & Management, pp. 46-50, Vol. 16 Issue 1, January 2013

[4] N. Tambey and ML Kothari, "Damping of power system oscillation with Unified Power Flow Controller," in Proceedings of IEE Gene., Trans. & Dist., vol. 150, no. 2, 2003, pp. 129-140.

[5] Anu Rani Sam, P.Arul," Transient Stability Enhancement of Multi-machine Power System Using UPFC and SSSC ", International Journal of Innovative Technology and Exploring Engineering, pp. 77-81, Vol. 3 Issue 5, Oct. 2013.

[6] V. Ganesh1, K. Vasu, K. Venkata Rami Reddy, M. Surendranath Reddy and T. GowriManohar," IMPROVEMENT OF TRANSIENT STABILITY THROUGH SVC", International Journal of Advances in Engineering & Technology, pp. 56-66, Vol. 5, Issue 1, Nov. 2012.

[7] A. Jalilvant, A. Safari and R. Aghmasheh, "Design of State Feedback Stabilizer for Multi-Machine Power System Using PSO Algorithm", Proc. IEEE International Multi-Topic Conference, Dec. 2008.

[8] M. Jazaeri, M. Ehsan, H.F. Wang and A.T. Johns, "Dynamic Interaction of Multiple Multi-Functional UPFC in Power Systems", Scientia Iranica, Vol. 9, No. 4, pp. 346-353, Oct. 2002.

[9] Hasan FayaziBoroujeni, MeysamEghtedari, Ahmad Memaripour and ElaheBehzadipour," Low frequency oscillation at a multi machine environment by using UPFC tuned based on Simulated Annealing", Indian Journal of Science and Technology, pp. 1630-1634, Vol. 4, No. 12, Dec. 2011.

[10] H. Shayeghi, H. A. Shayanfar, S. Jalilzadeh and A. Safari, "Design of output feedback UPFC controllers for damping of electromechanical oscillations using PSO", Energy Convers Manage, vol. 50, **(2009)**, pp. 2554-2561.

[11] Jiang X, Chow JH, Edris A and Fardanesh B (2010) Transfer path stability enhancement by voltage sourced converter-based FACTS controllers. IEEE transactions on Power Delivery.25, 1019 –1025.

[12] R. Kanimozhi and K. Selvi, "A Novel Line Stability Index for Voltage Stability Analysis and Contingency Ranking in Power System Using Fuzzy Based Load Flow", J Electrical Engineering Technology,  pp. 694-703, , Vol. 8, No. 4, 2013

[13] V. Jayasankar, N. Kamaraj, N. Vanaja, "Estimation of voltage stability index for power system employing artificial neural network technique and TCSC placement", Elsevier Neuro computing 73, pp. 3005-3011, 2010.

[14] W. Zhong, S. Li and F. Qian, "$\theta$-PSO: a new strategy of particle swarm optimization", J. Zhejiang Univ. Sci., vol. 9, no. 6, **(2008)**, pp. 786-790.

[15] Amin Safari," θ-PSO Algorithm for UPFC Based Output Feedback Damping Controller", International Journal of Control and Automation, pp. 33-46, Vol. 6, No. 1 Feb. 2013

[16] H. Shayeghi, H. A. Shayanfar, S. Jalilzadeh and A. Safari, "A quantum particle swarm optimizer for the tuning of Unified Power Flow Controller", Energy Conver. Manage, Vol. 51, **(2010)**, pp. 2299-2306.

[17] Mohammed .A. Mohammed, "FACTS Modeling in Load Flow Studies", M.Sc. Thesis, Assuit University, Assuit, Egypt, 2008.

[18] M.Z.EL-Sadek, A. Ahmed, M. A. Mohammed, "Advanced Modeling of FACTS in Newton Power Flow", Journal of Engineering Sciences, Assuit University, Vol. 35,No. 6, PP. 1467-1479, Nov. 2007

[19] M.Z.EL-Sadek, A. Ahmed, M. A. Mohammed, "Incorporating of GUPFC in load flow studies", 5 (fifth) Saudi technical conference and exhibition (5 fifth stcex), king faaial auditorium, Riyadh, Saudi Arabia, vol. 103, pp. 525-539, jaunty 11-14, 2009

[20] M.Z.EL-Sadek, A. Ahmed, M. A. Mohammed, "Incorporating of IPFC in load flow studies", 5 (fifth) Saudi technical conference and exhibition (5 fifth stcex), king faaial auditorium, Riyadh, Saudi Arabia, vol. 103, pp. 214-225, January 11-14, 2009

[21] G.El-Saady, A. Ahmed, EL Noby, M. A. Mohammed," Optimal Location of UPFC in Power Systems ", Proceeding of the 15th International Middle-East Power Systems Conference (MEPCON'12), Alexandria-Egypt, pp. 522-527, December 23-25, 2012.

[22] Power Systems Test Case Archive: University of Washington, Available from http:// www.ee.washington.edu/research/pstca/,2003.

## تحسين ثبات نظام القوى متعدد المولدات في مواجهة الإضطرابات العابرة بواسطة الاختيار الأمثل لمكان وقيم معاملات متحكمات سريان القدرة الموحدة وذلك بطريقة الوجه الزاوي للحشد المثالي للجزيئات

### الملخص العربى

قدم البحث نمذجة رياضية للإختيار الأمثل لقيم معملات متحكمات سريان القدرة الموحدة بالتزامن مع الإختيار الأمثل لمكانها في نظام القوى واستخدم تقليل مؤشرا جديدا لثبات الجهود كدالة هدفية لذلك وذلك بطريقة الوجه الزاوي للحشد المثالي للجزيئات كما قدم أيضا إجراء مقترحا للتحكم المثالي المتناسق لمتحكمات سريان القدرة الموحدة ومثبتات التذبذب في نظام القوى متعدد المولدات وذلك لتحقيق ثباتية النظام والإخماد المثالي للإضطرابات العابرة وتم دراسة ذلك علي نظامين IEEE14-bus system و -IEEE30 bus system وقد أثبتت النتائج أن نظام القوي يصبح أكثر إستقرارا في وجود متحكمات سريان القدرة الموحدة وذلك إذا ما تم إختيار الأمثل لمكانه ومعاملاته وأيضا المقدرة العالية لطريقة الوجه الزاوي للحشد المثالي للجزيئات لعملية الاختيار الأمثل.